Polychromatic Tomography of High Energy Density Plasmas

T. Nagayama[1], R. Mancini[1], R. Florido[1], R. Tommasini[2], J. Koch[2], J. Delettrez[3], S. Regan[3], V. Smalyuk[3]

[1]Physics Department, University of Nevada, Reno
[2]Lawrence Livermore National Laboratory
[3]Laboratory for Laser Energetics, University of Rochester

OMEGA direct-drive implosions

- The amount of Ar has to be very small:
  - Not to change the hydrodynamics
  - To keep the optical depth of the Heβ and Lyβ (n=3-1 transitions) small
- Laser:
  - 60 beams, several pulse shapes
  - Smoothing: 2D-SSD/DPP-SG4/DPR
- Three identical DDMMI instruments:
  - DDMMI ≡ Direct-Drive Multi-Monochromatic x-ray Imager
  - Fielded along 3 quasi-orthogonal lines of sight (TIM3/TIM4/TIM5)
  - Record a collection of, gated, spectrally-resolved x-ray images of the implosion core

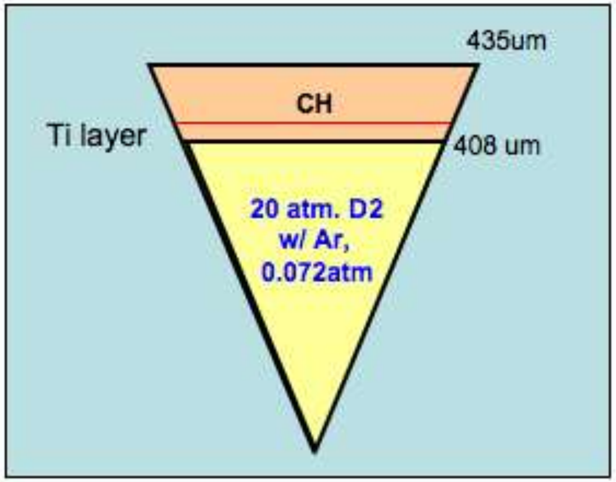

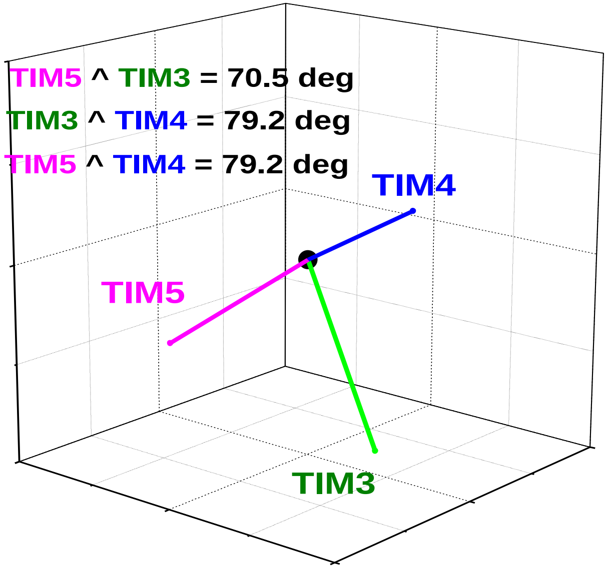

Spectrally-resolved core imaging with DDMMI

DDMMI ≡ Direct-Drive Multi-Monochromatic x-ray Imager

- A pinhole-array coupled to a multi-layer Bragg mirror produces many quasi-monochromatic core images, each one characteristic of a slightly different photon energy range[1,2]

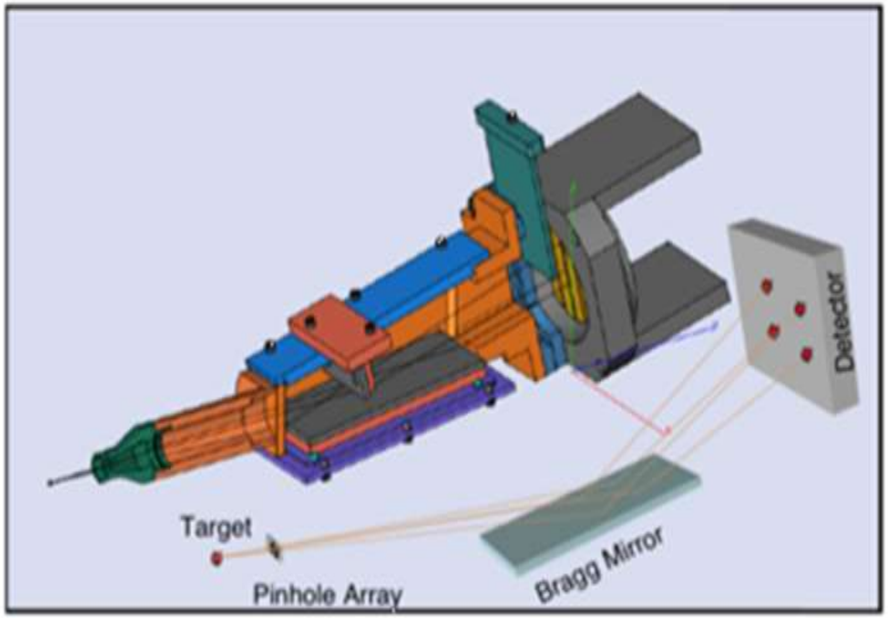

Pinhole is snout-mounted and placed as close as possible to target to maximize signal and spatial resolution, for a given pinhole aperture.

- pinhole array-target distance = 31.5mm
- target-mirror distance = 188mm
- Pinhole diameter = 10μm
- detector = gated X-ray framing cameras
- images recorded with CCD or film.
- Magnification, M = 8.5X.

[1]R. Tommasini, J. Koch, N. Izumi, L. Welser, R. Mancini, J. Delettrez, S. Regan and V. Smalyuk, Rev. Sci. Instrum. 77, 10E303 (2006);
[2]T. Nagayama, R. Mancini, R. Florido, R. Tommasini, J. Koch, J. Delettrez, S. Regan, V. Smalyuk, L. Welser, and I. Golovkin, Rev. Sci. Instrum. 79, 10E921 (2008);

DDMMI data: spectrally resolved images

- Collection of gated, spectrally-resolved images
- Time increases from F1 to F4
- Photon energy axis increases from left to right
- Resolution:
  - Spatial: Δx = 10 μm
  - Spectral: $E/\Delta E$ = 150
  - Frame separation = 100 ps

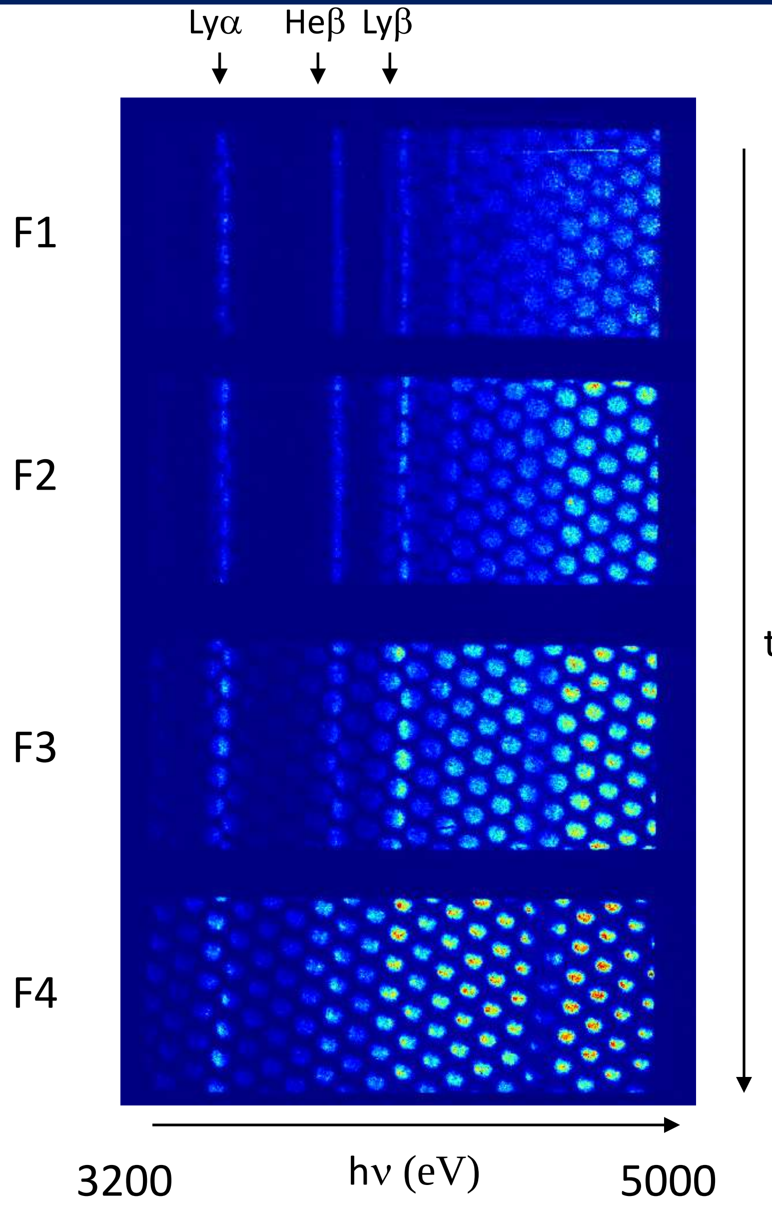

DDMMI data: spectrally resolved images

- Collection of gated, spectrally-resolved images
- Time increases from F1 to F4
- Photon energy axis increases from left to right
- Resolution:
  - Spatial: $\Delta x = 10\ \mu m$
  - Spectral: $E/\Delta E = 150$
  - Frame separation = 100 ps

Narrow-band (Heβ)

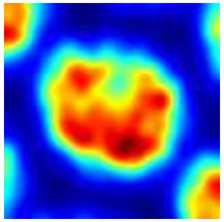

Space-integrated

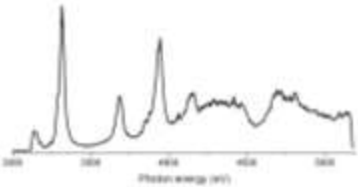

Broad-band

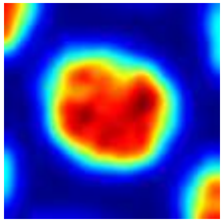

Space-resolved

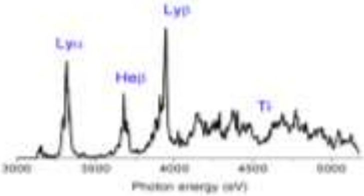

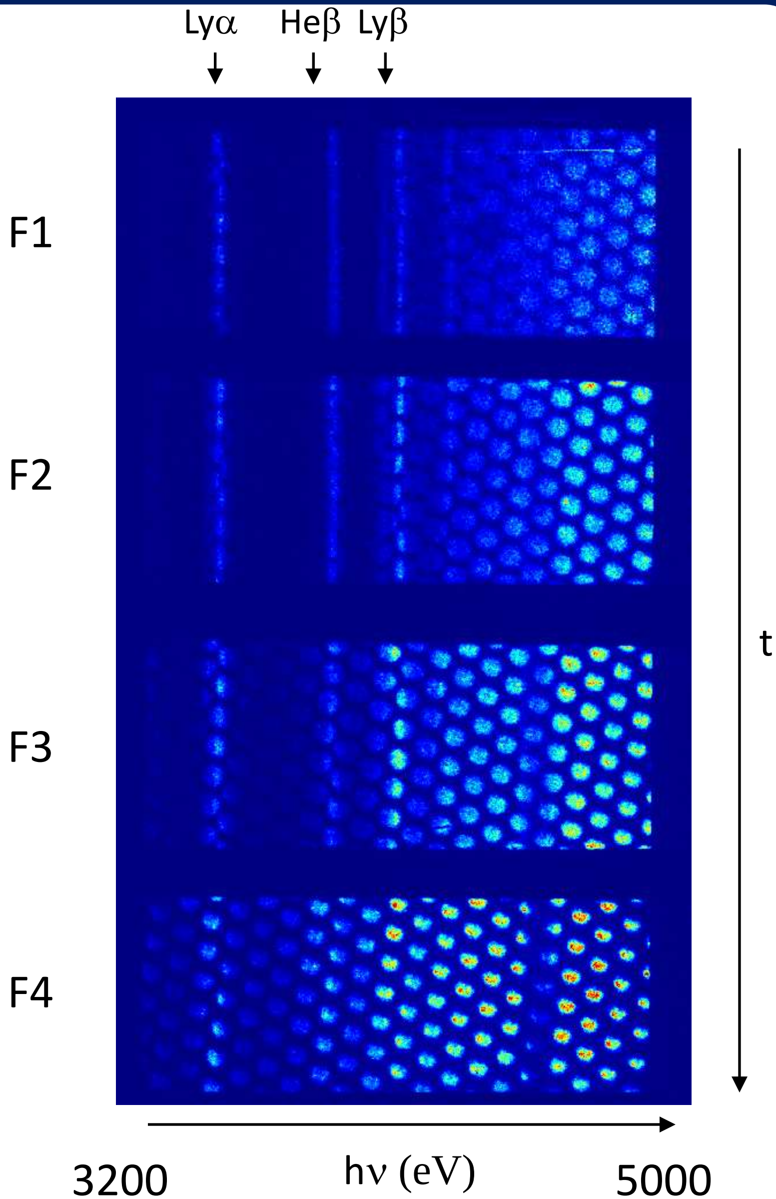

Data processing: space-resolved spectrum (SRS)

- What if we pick up the contributions only from a selected region of the core image?

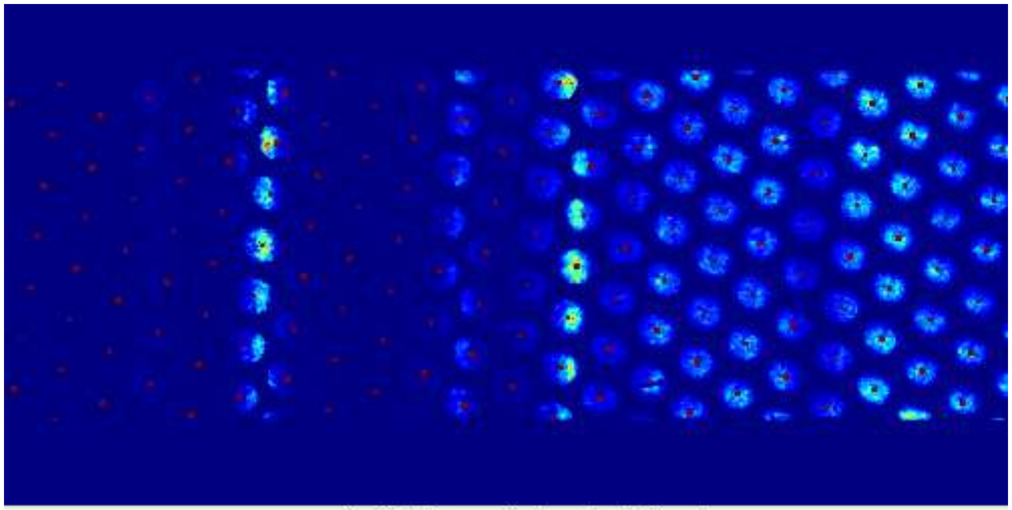

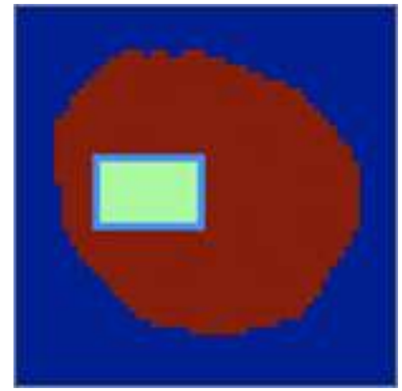

Mask of selected region

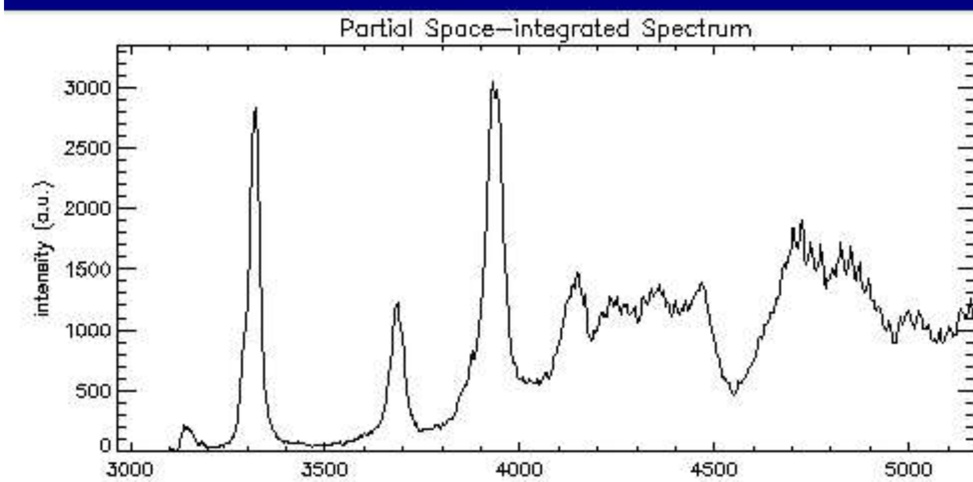

Data processing: space-resolved spectrum (SRS)

- What if we pick up the contributions only from a selected region of the core image?
- The result is a space-resolved spectrum integrated along a chord in the core

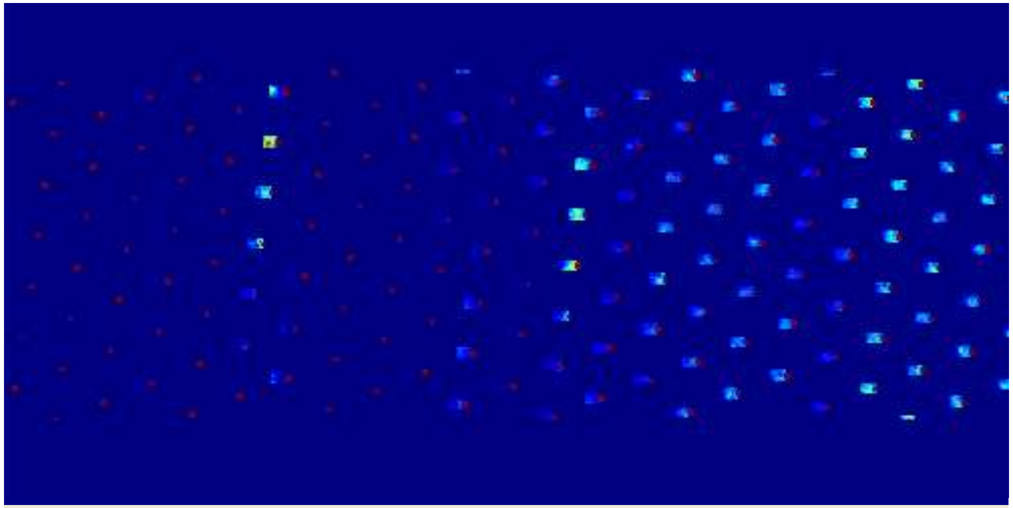

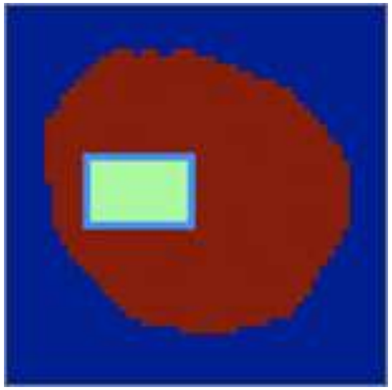

Mask of selected region

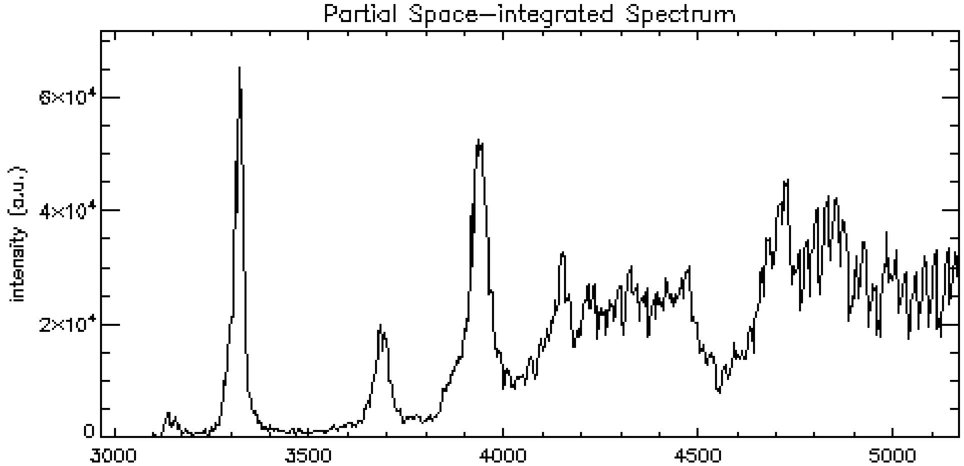

Limitations:
- Signal-to-noise ratio
- Spatial resolution

Interpretation of SRS

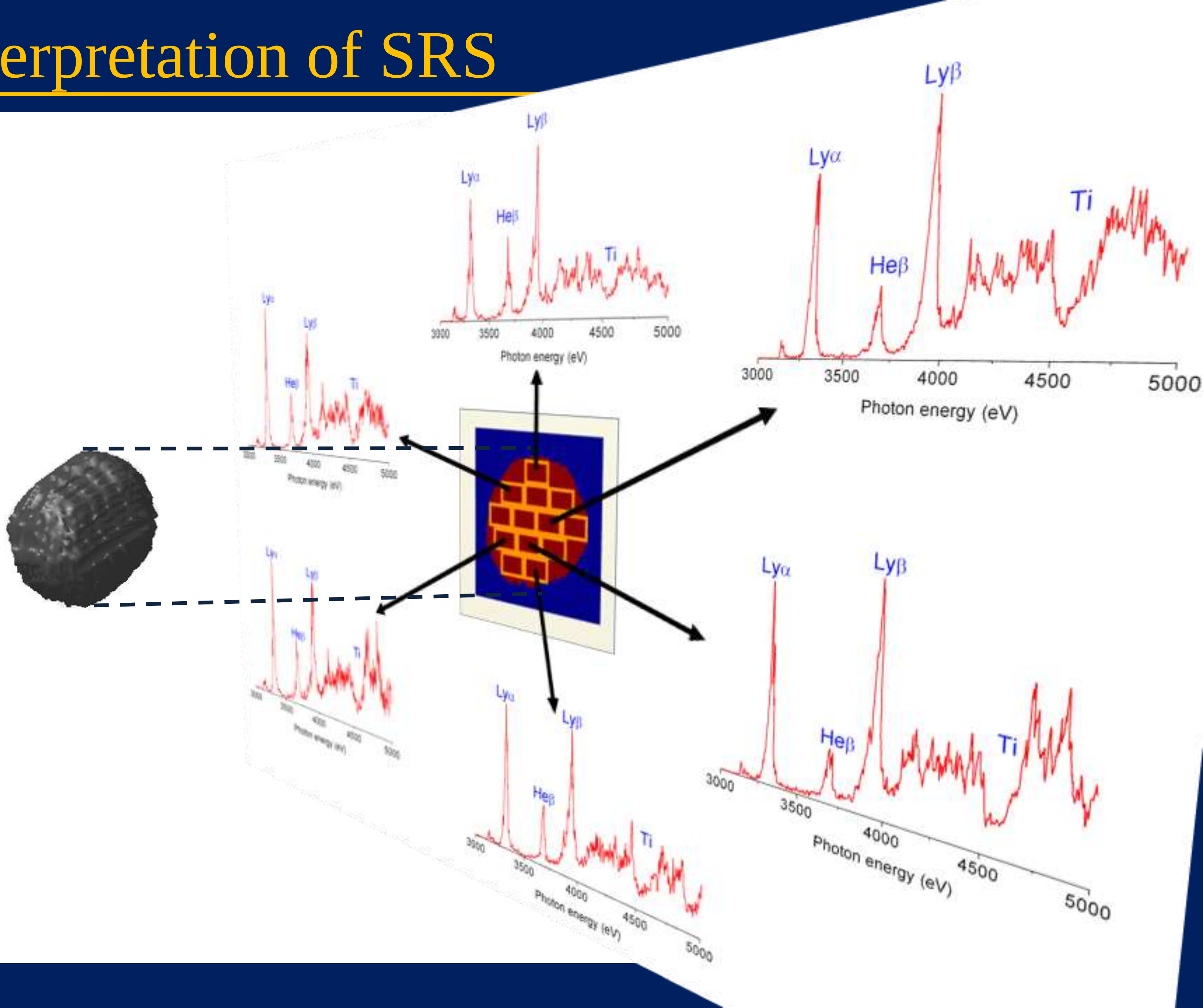

Interpretation of SRS

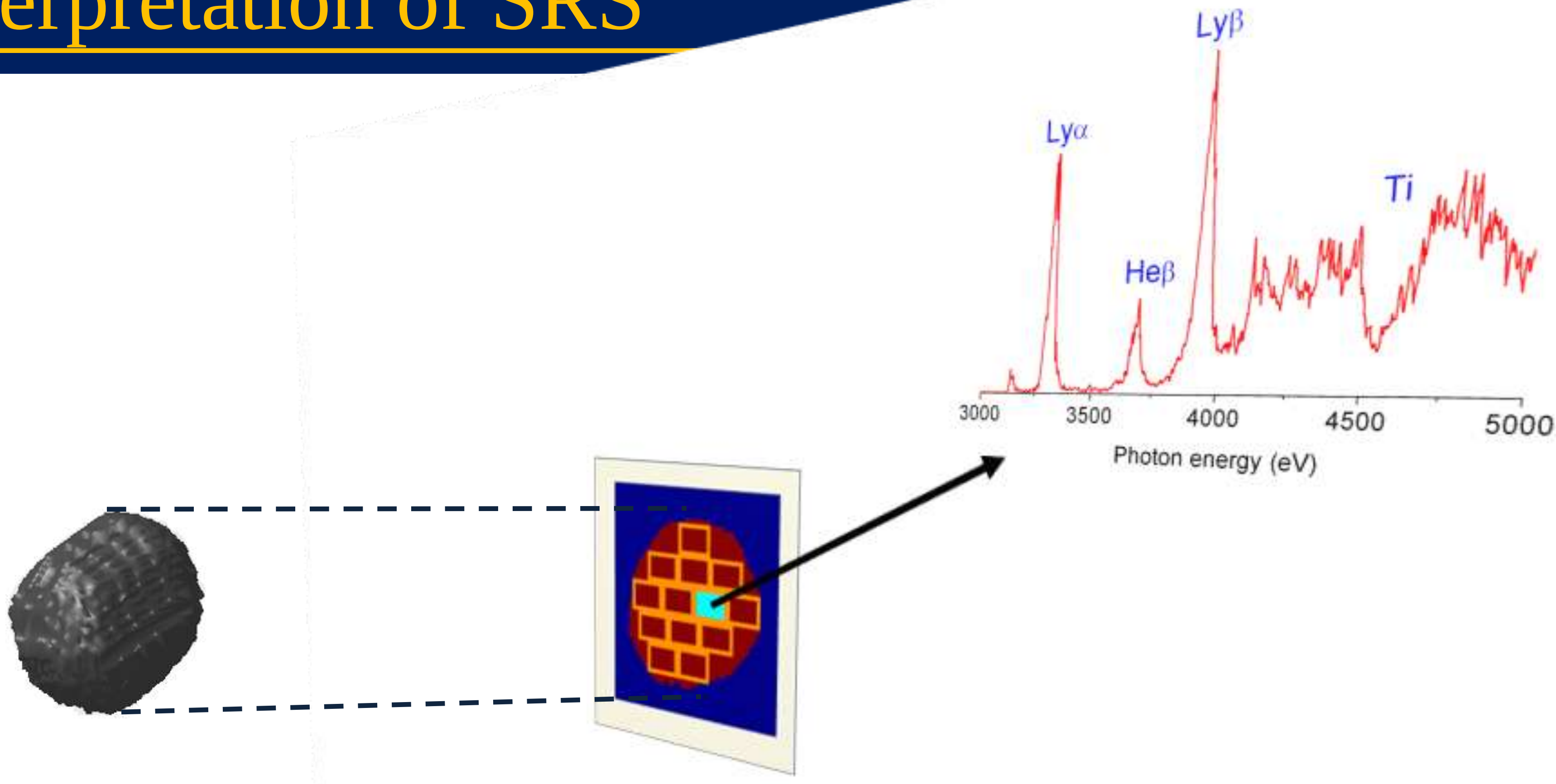

Interpretation of SRS

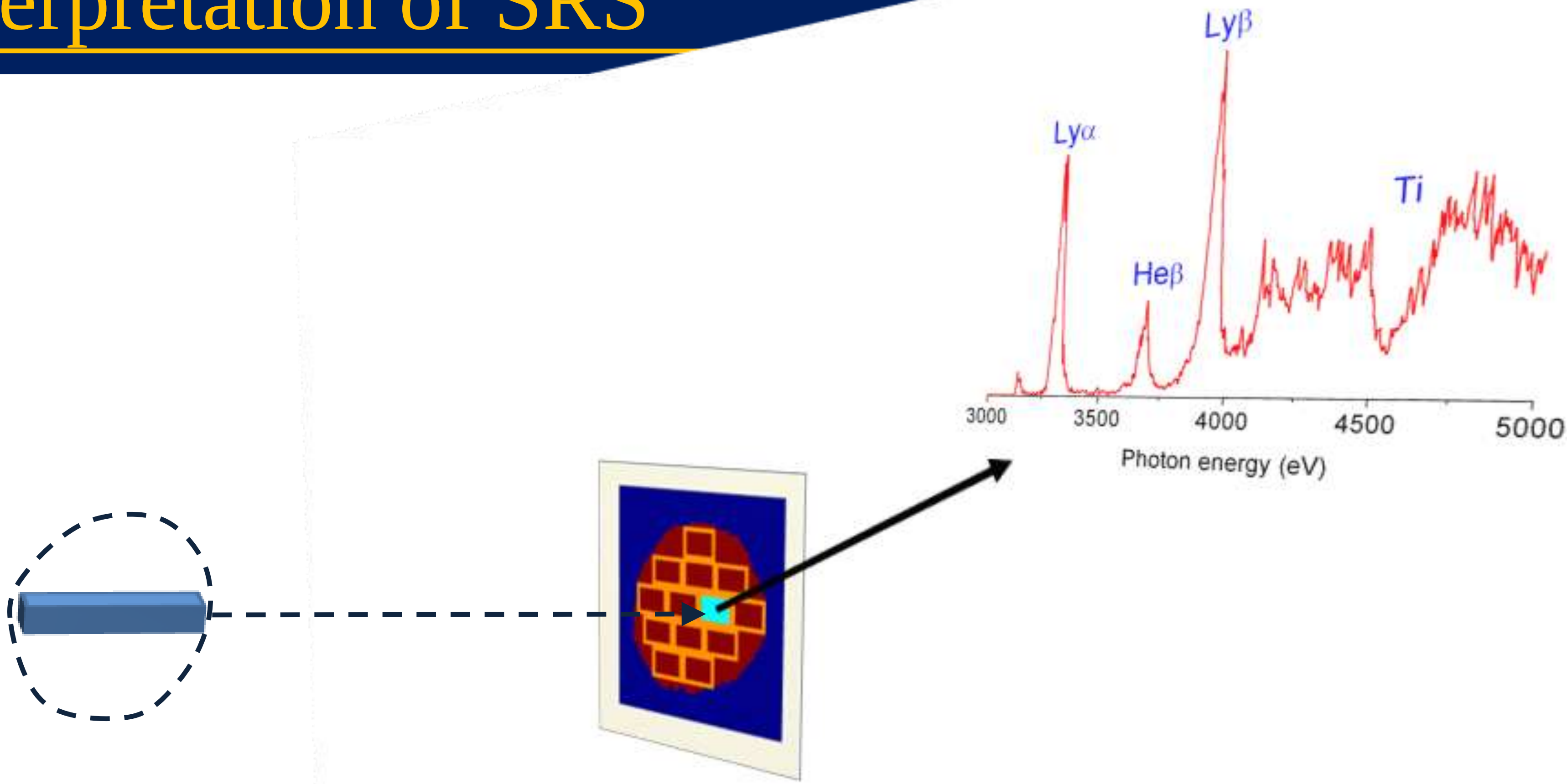

- Each space-resolved spectrum has temperature and density information integrated along chord parallel to LOS and perpendicular to the image plane

Interpretation of SRS

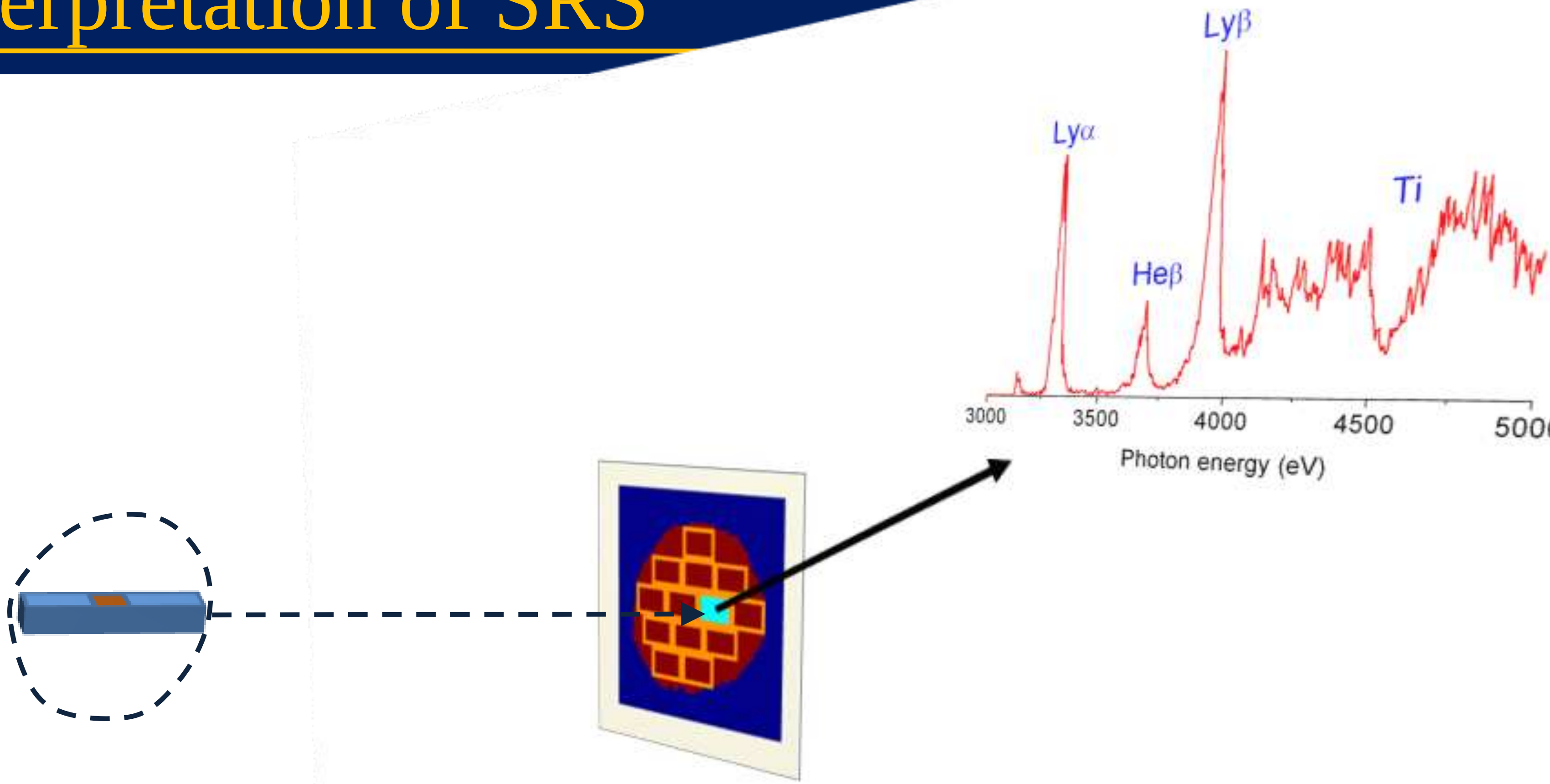

- Each space-resolved spectrum has temperature and density information integrated along chord parallel to LOS and perpendicular to the image plane

Interpretation of SRS

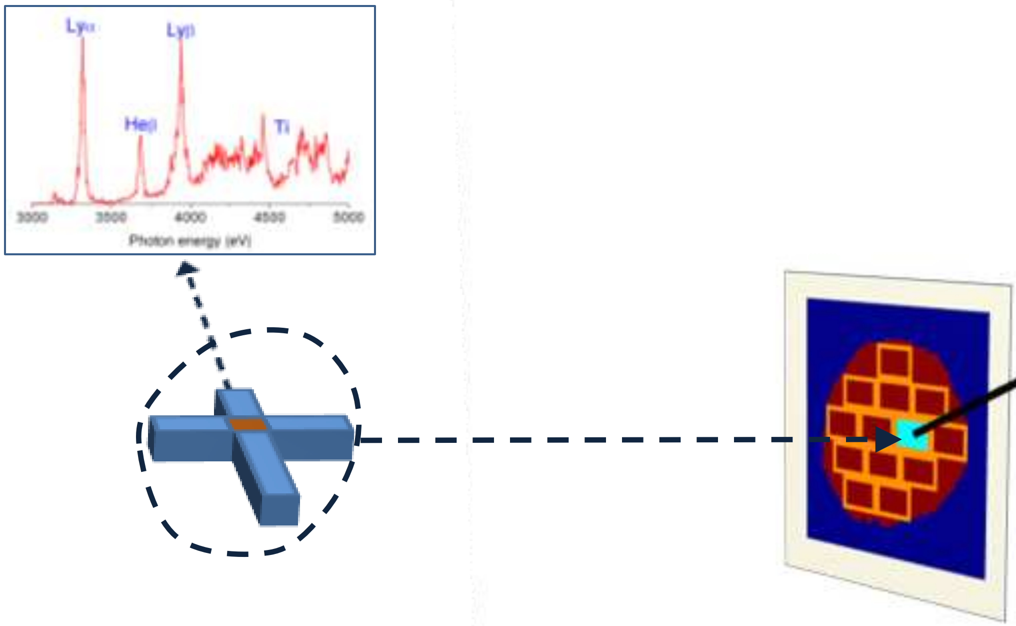

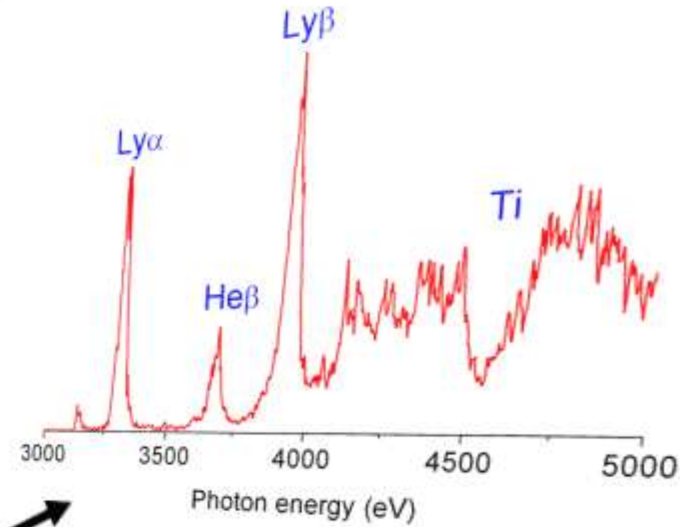

- Each space-resolved spectrum has temperature and density information integrated along chord parallel to LOS and perpendicular to the image plane
- Each spatial region is located at the intersection of three chords
- Spatial regions are constrained by their contributions to spatially-resolved spectra recorded along three LOS

3 LOS, but multiple λ

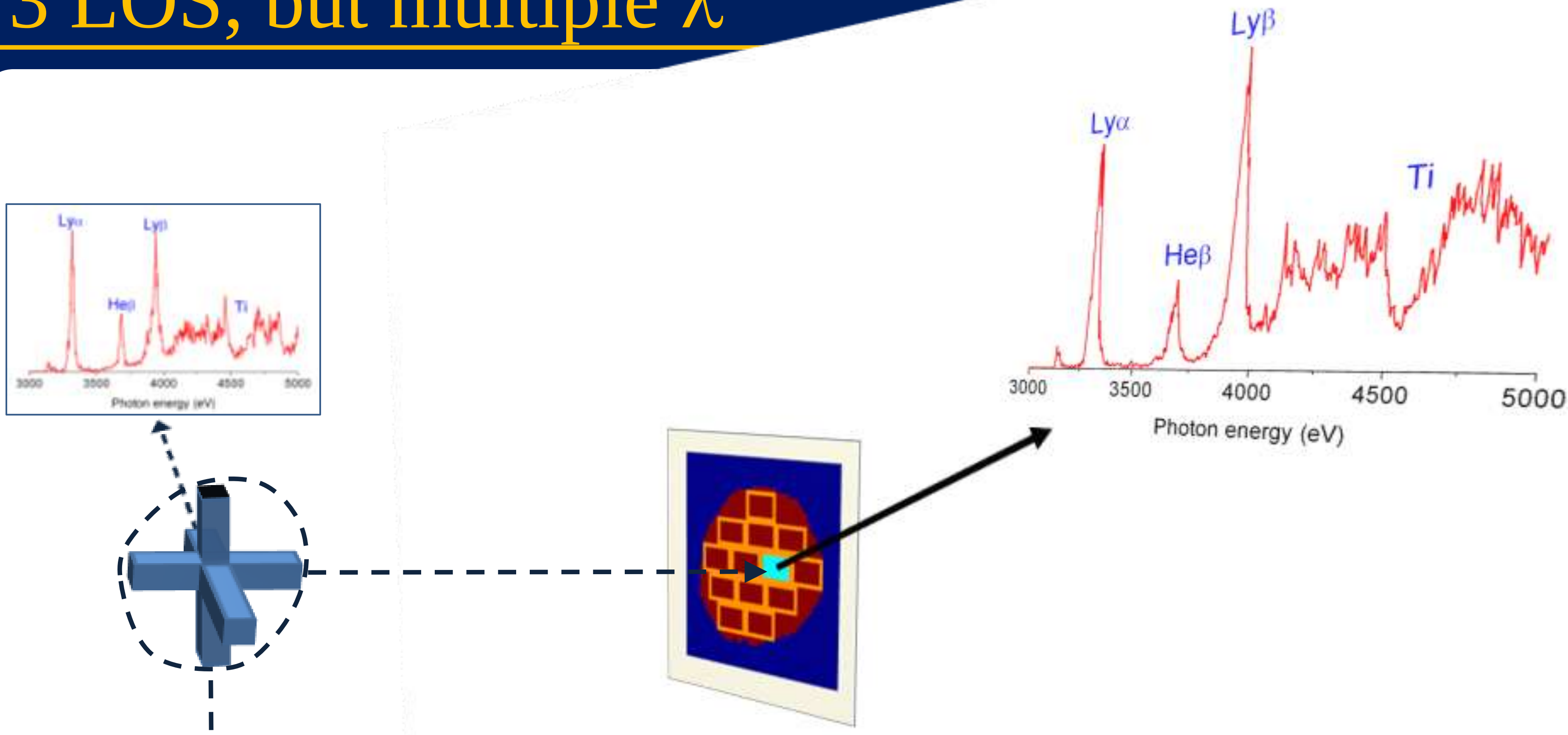

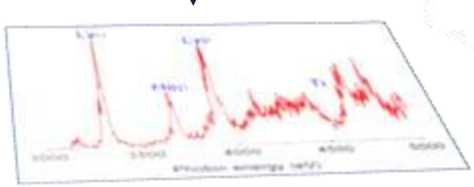

- Each space-resolved spectrum has temperature and density information integrated along chord parallel to LOS and perpendicular to the image plane
- Each spatial region is located at the intersection of three chords
- Spatial regions are constrained by their contributions to spatially-resolved spectra recorded along three LOS

Modeling

- Physics model: T_e and N_e → SRS
  1. Detailed collisional-radiative atomic kinetics model
  2. Numerical integration of the radiation transport equation
- Search and reconstruction + model: SRS → T_e and N_e
  1. Pareto genetic algorithm (PGA)
     - Fast and robust search algorithm
     - Initialized by random number generator → unbiased
  2. Fine-tuning step
     - Least-squares minimization method
     - Refine the PGA results to the very best

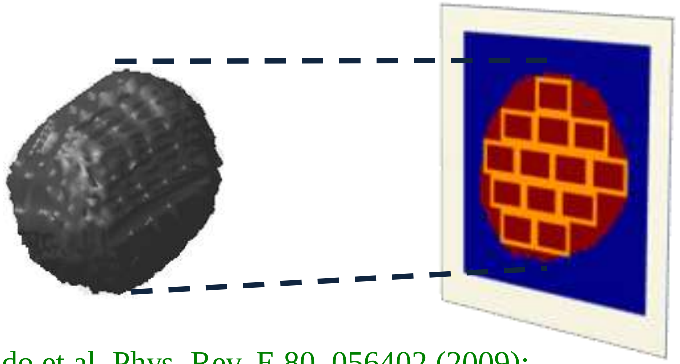

* R. Florido et al, Phys. Rev. E 80, 056402 (2009);

Modeling

- Physics model: T_e and N_e → SRS
  1. Detailed collisional-radiative atomic kinetics model
  2. Numerical integration of the radiation transport equation
- Search and reconstruction + model: SRS → T_e and N_e
  1. Pareto genetic algorithm (PGA)
     - Fast and robust search algorithm
     - Initialized by random number generator → unbiased
  2. Fine-tuning step
     - Least-squares minimization method
     - Refine the PGA results to the very best

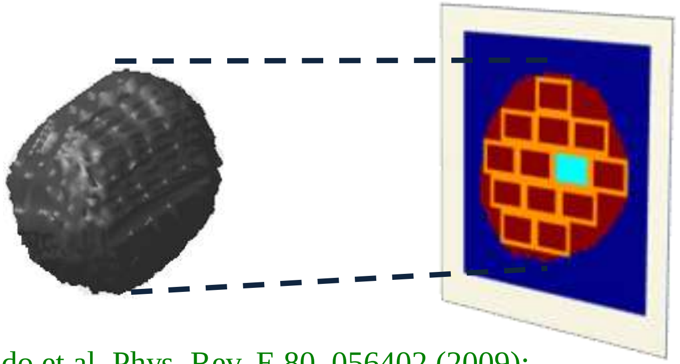

* R. Florido et al, Phys. Rev. E 80, 056402 (2009);

Modeling

- Physics model: T_e and N_e → SRS
  1. Detailed collisional-radiative atomic kinetics model
  2. Numerical integration of the radiation transport equation
- Search and reconstruction + model: SRS → T_e and N_e
  1. Pareto genetic algorithm (PGA)
     - Fast and robust search algorithm
     - Initialized by random number generator → unbiased
  2. Fine-tuning step
     - Least-squares minimization method
     - Refine the PGA results to the very best

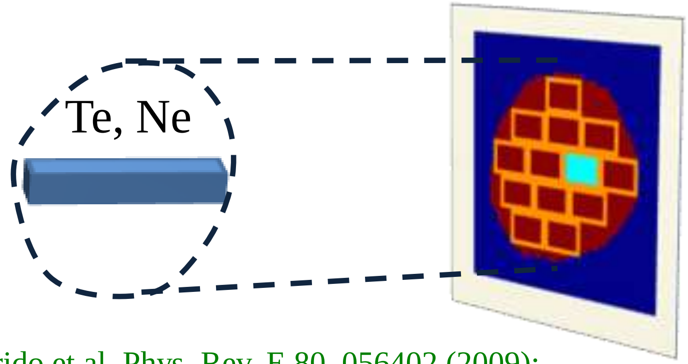

* R. Florido et al, Phys. Rev. E 80, 056402 (2009);

Modeling

- Physics model: T_e and N_e → SRS
    1. Detailed collisional-radiative atomic kinetics model
    2. Numerical integration of the radiation transport equation
- Search and reconstruction + model: SRS → T_e and N_e
    1. Pareto genetic algorithm (PGA)
        - Fast and robust search algorithm
        - Initialized by random number generator → unbiased
    2. Fine-tuning step
        - Least-squares minimization method
        - Refine the PGA results to the very best

$$\frac{dI_\nu}{dx} = \varepsilon_\nu - I_\nu \kappa_\nu \quad \Rightarrow \quad I_\nu = \int_{rear}^{front} \varepsilon_\nu(x') e^{-\tau_\nu(x')} dx'$$

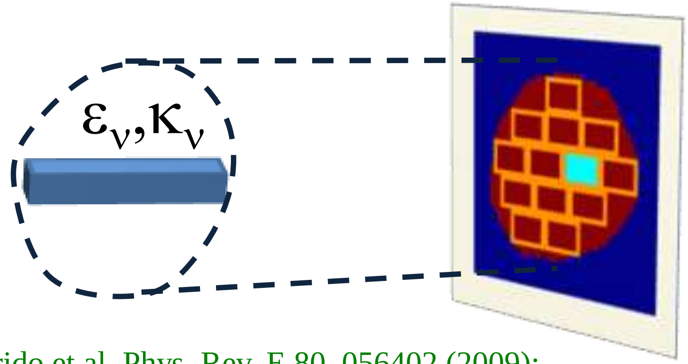

* R. Florido et al, Phys. Rev. E 80, 056402 (2009);

Modeling

- Physics model: T_e and N_e → SRS
  1. Detailed collisional-radiative atomic kinetics model
  2. Numerical integration of the radiation transport equation
- Search and reconstruction + model: SRS → T_e and N_e
  1. Pareto genetic algorithm (PGA)
     - Fast and robust search algorithm
     - Initialized by random number generator → unbiased
  2. Fine-tuning step
     - Least-squares minimization method
     - Refine the PGA results to the very best

$$\frac{dI_\nu}{dx} = \varepsilon_\nu - I_\nu \kappa_\nu \quad \Rightarrow \quad I_\nu = \int_{rear}^{front} \varepsilon_\nu(x')e^{-\tau_\nu(x')}dx'$$

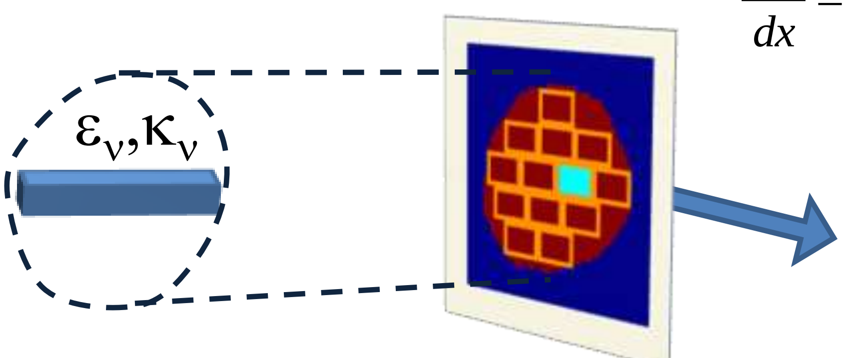

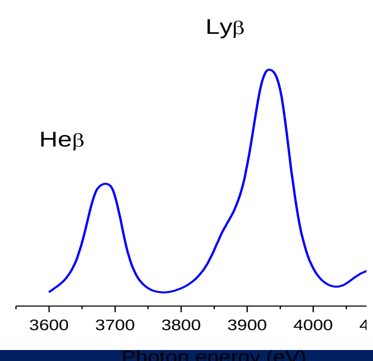

* R. Florido et al, Phys. Rev. E 80, 056402 (2009);

Modeling

- Physics model: T_e and N_e → SRS
  1. Detailed collisional-radiative atomic kinetics model
  2. Numerical integration of the radiation transport equation
- Search and reconstruction + model: SRS → T_e and N_e
  1. Pareto genetic algorithm (PGA)
     - Fast and robust search algorithm
     - Initialized by random number generator → unbiased
  2. Fine-tuning step
     - Least-squares minimization method
     - Refine the PGA results to the very best

$$\frac{dI_\nu}{dx} = \varepsilon_\nu - I_\nu \kappa_\nu \quad \Rightarrow \quad I_\nu = \int_{rear}^{front} \varepsilon_\nu(x') e^{-\tau_\nu(x')} dx'$$

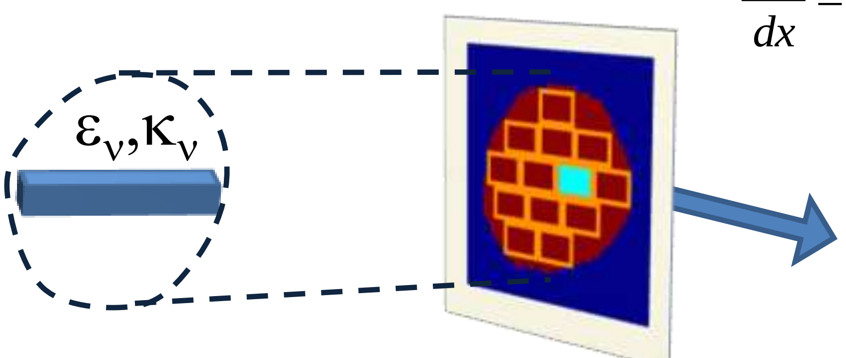

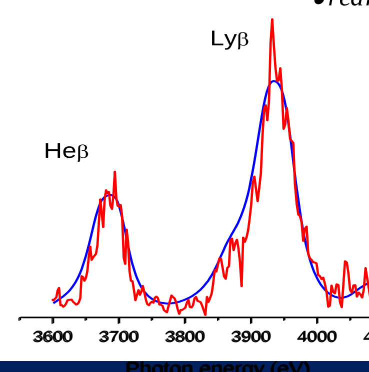

* R. Florido et al, Phys. Rev. E 80, 056402 (2009);

Results: OMEGA shot 49956 frame 3

- A total of 141 SRS were used to extract T_e and N_e spatial structure
- Te tends to be larger in central region Ne in the periphery
- 3D asymmetries in the spatial structures are observed

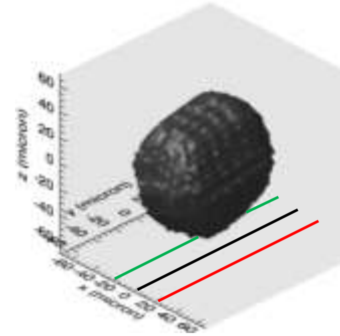

x = -21 μm x = 0 μm x = 21 μm

Te (eV)

Ne (cm^{-3})

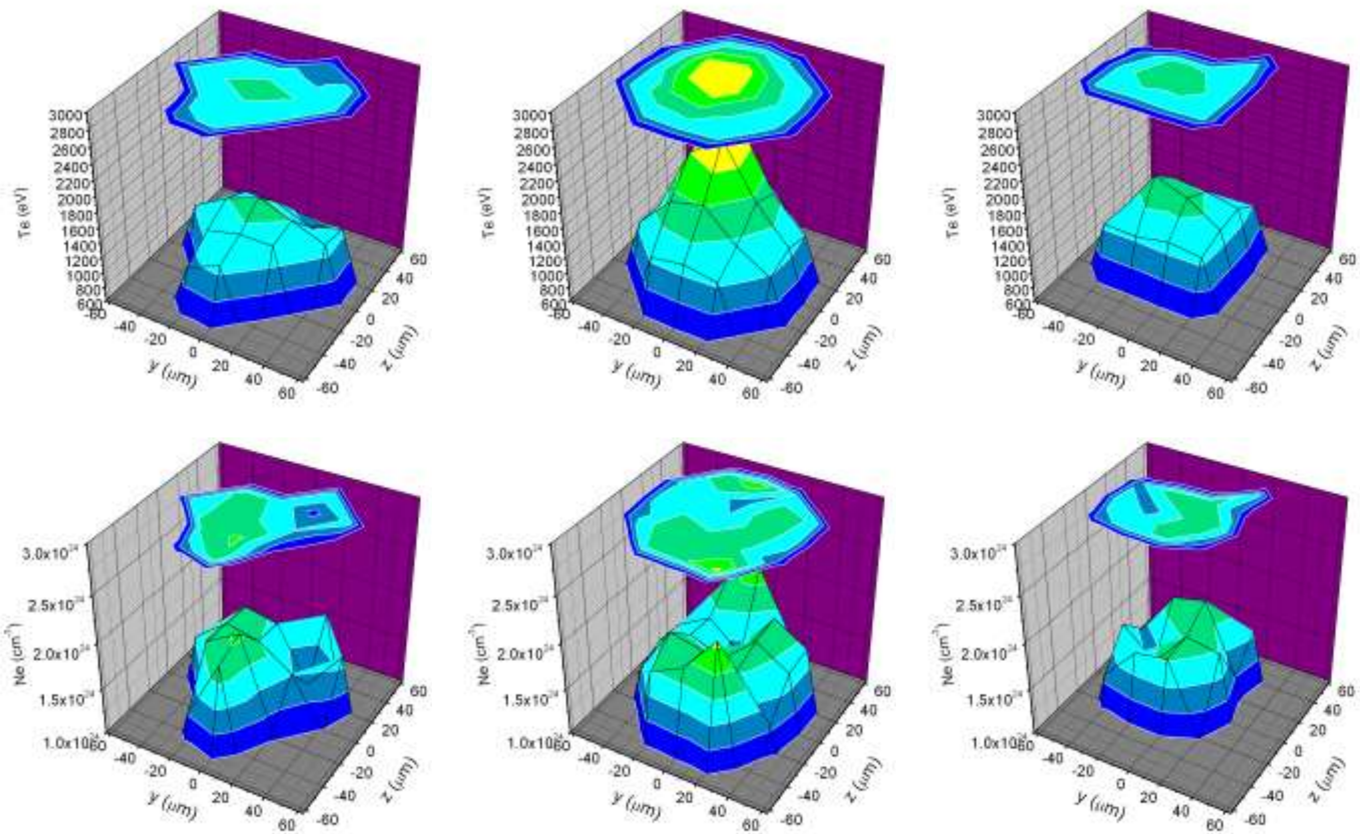

Results: OMEGA shot 49956 frame 3

- A total of 141 SRS were used to extract T_e and N_e spatial structure
- Te tends to be larger in central region Ne in the periphery
- 3D asymmetries in the spatial structures are observed

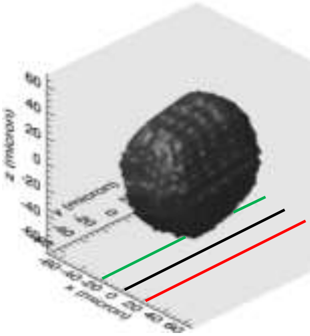

x = -21 μm   x = 0 μm   x = 21 μm

Te (eV)

Ne (cm^{-3})

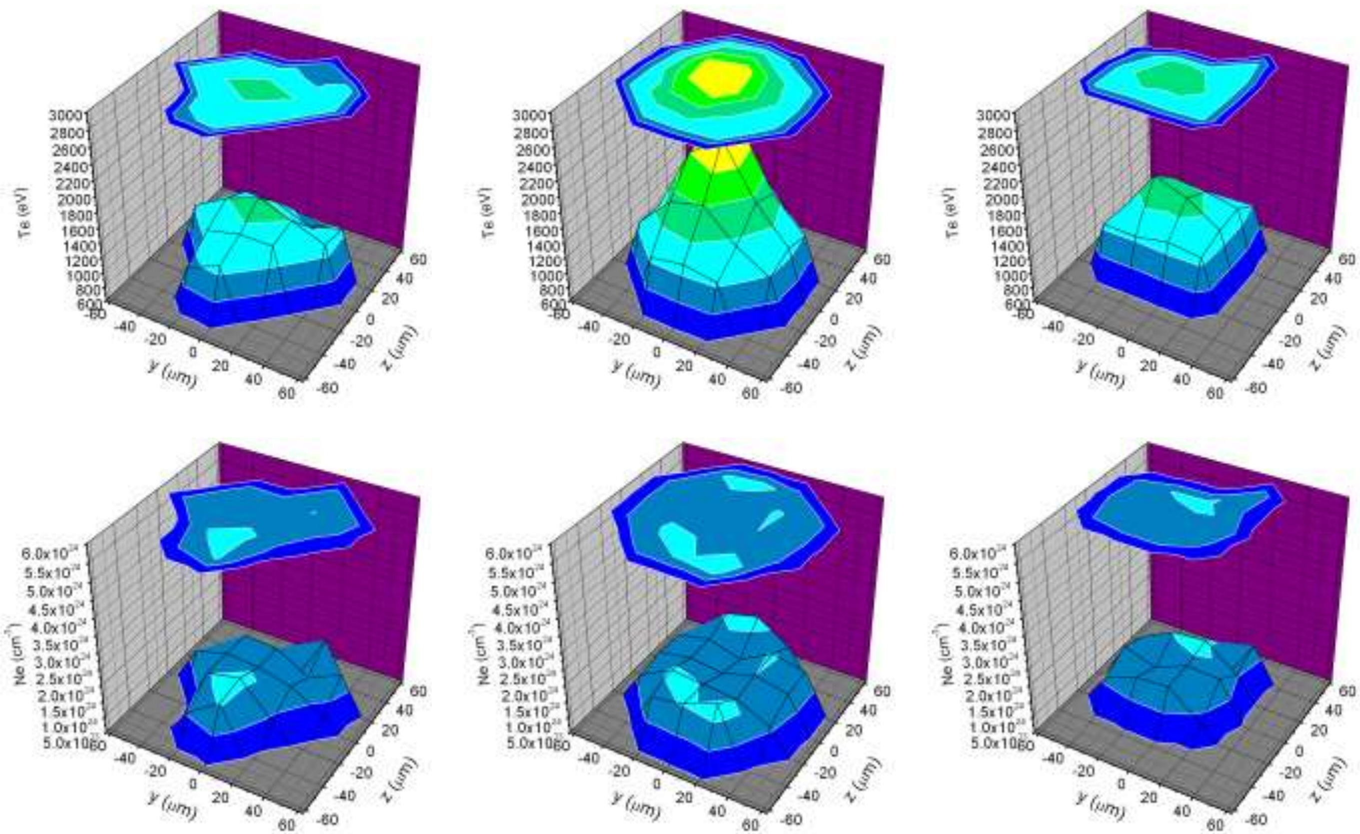

Results: OMEGA shot 49956 frame 4

- A total of 85 SRS were used to extract T_e and N_e spatial structure
- Frame 4 is close to stagnation and the volume is smaller
- Ne has increased while Te has decreased

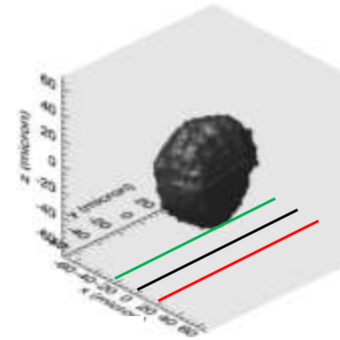

x = -21 μm | x = 0 μm | x = 21 μm

Te (eV)

Ne (cm^{-3})

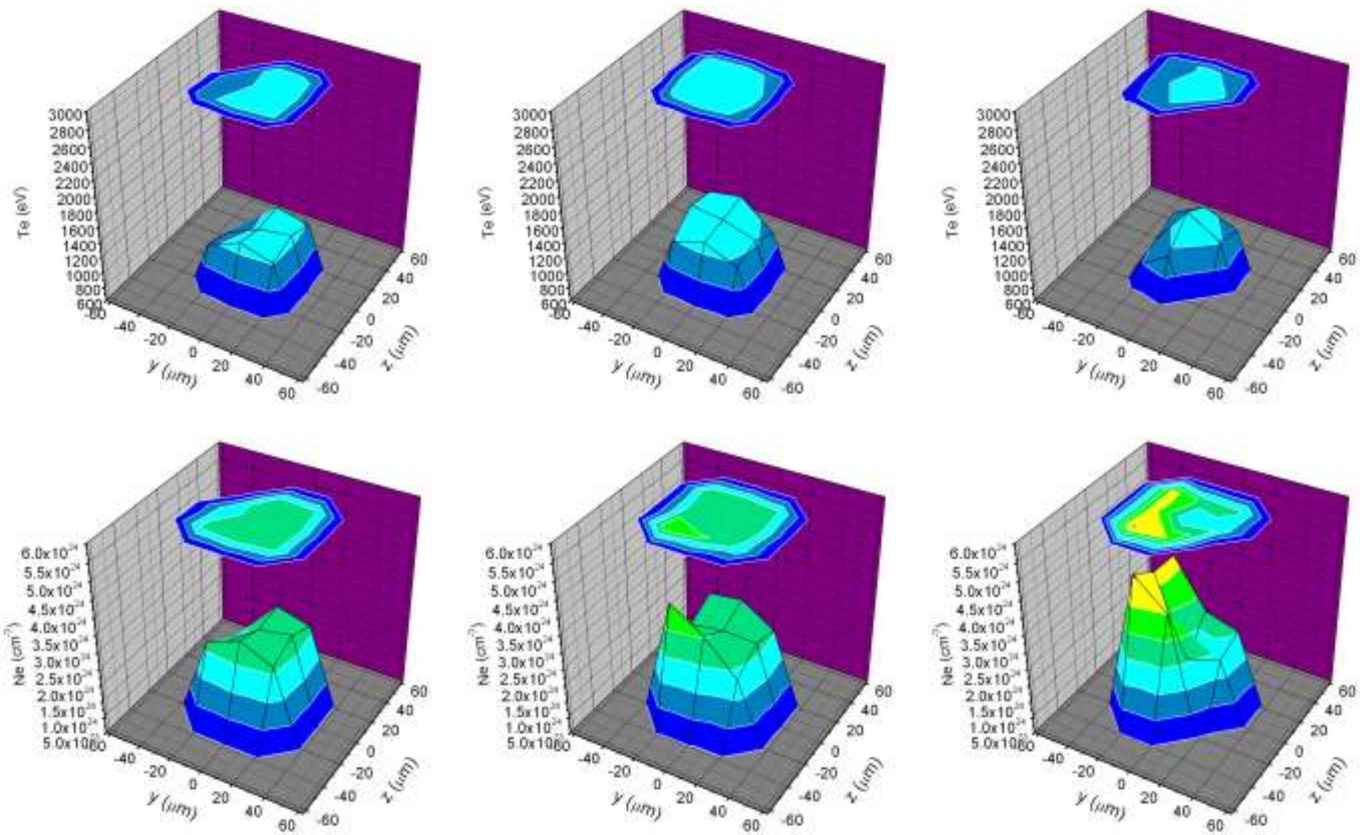

Results: OMEGA shot 49956 (Pe evolution)

- Pressure distribution is computed based on the Te and Ne distributions
- Frame 3 shows larger gradient in the pressure distribution than Frame 4
- As imploded, the core becomes more isobaric

x = -21 μm   x = 0 μm   x = 21 μm

Frame 3

Frame 4

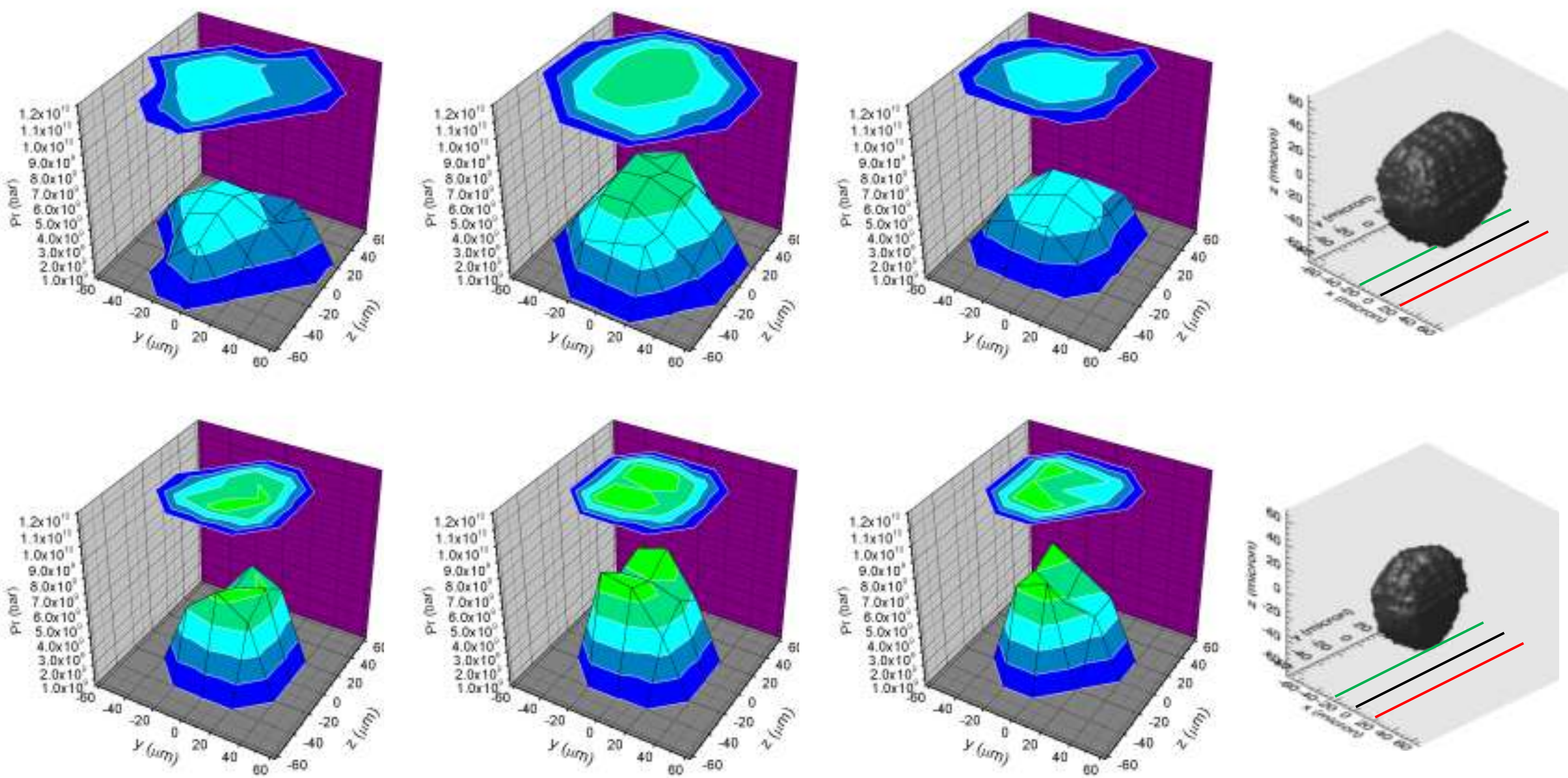

Conclusions

- T_e and N_e spatial distributions have been extracted from the analysis of space-resolved spectra (SRS) obtained from spectrally-resolved images recorded with three-identical DDMMI instruments fielded along quasi-orthogonal directions

- Analysis method:
  - Two step search and reconstruction: PGA followed up by fine-tuning
  - Method was tested with the synthetic test case
  - This method can be interpreted as polychromatic tomography; number of LOS is limited but there are multiple wavelengths associated with each LOS

- Work in progress:
  - Extract mixing distribution
  - Error estimation
  - Further synthetic data test cases
  - Comparison with 2D/3D hydrodynamics simulation

Work supported by DOE/NLUF Grant DE-FG52-09NA29042, and LLNL